High-sensitivity vibrational imaging with frequency modulation coherent anti-Stokes Raman scattering (FM CARS) microscopy

Feruz Ganikhanov, Conor L. Evans, Brian G. Saar, and X. Sunney Xie

Department of Chemistry and Chemical Biology, Harvard University, 12 Oxford Street, Cambridge, Massachusetts 02138

Received January 9, 2006; revised March 22, 2006; accepted March 23, 2006; posted April 3, 2006 (Doc. ID 67105)

We demonstrate a new approach to coherent anti-Stokes Raman scattering (CARS) microscopy that significantly increases the detection sensitivity. CARS signals are generated by collinearly overlapped, tightly focused, and raster scanned pump and Stokes laser beams, whose difference frequency is rapidly modulated. The resulting amplitude modulation of the CARS signal is detected through a lock-in amplifier. This scheme efficiently suppresses the nonresonant background and allows for the detection of far fewer vibrational oscillators than possible through existing CARS microscopy methods. © 2006 Optical Society of America

OCIS codes: 110.0180, 180.5810, 300.6230, 190.4380.

CARS microscopy has matured into a powerful technique[1] with applications in the fields of biomedical imaging[2] and cell biology.[3] CARS is a third-order nonlinear optical process requiring pump and Stokes fields, with frequencies ω_p and ω_s, respectively. When the difference frequency between these fields is tuned to the frequency of a Raman-active molecular vibration ($\Omega=\omega_p-\omega_s$), a strong anti-Stokes signal is generated at frequency $\omega_{as}=2\omega_p-\omega_s$. CARS microscopy provides information about the intrinsic vibrational resonances of a sample, allowing for label-free, chemically specific imaging.

However, there is also a nonresonant contribution to the CARS signal from the sample that does not carry chemically specific information, which can distort and even overwhelm the resonant signal of interest. The CARS response originates from the third-order nonlinear susceptibility, which is the sum of a resonant contribution, $\chi_R^{(3)}(\Omega)$, and a nonresonant electronic component, $\chi_{NR}^{(3)}$. The total detected CARS signal is proportional to

$$I_{CARS}(\Omega) \propto |\chi_R^{(3)}(\Omega)+\chi_{NR}^{(3)}|^2 = |\chi_R^{(3)}(\Omega)|^2+(\chi_{NR}^{(3)})^2+2\,\mathrm{Re}\{\chi_R^{(3)}(\Omega)\}\chi_{NR}^{(3)}. \quad (1)$$

The frequency dependence of the three terms on the right-hand side of relation (1) is shown in Fig. 1a. The nonresonant term can make it difficult to identify the chemically selective contributions to an image. This is especially true when imaging biological materials, as the aqueous environment gives rise to a substantial nonresonant response.

Approaches such as epi-CARS, polarization-sensitive detection, and time-resolved CARS can eliminate the nonresonant background but have the disadvantage of severely attenuating the resonant signal.[1] Multiplex CARS imaging with a broadband femtosecond source[1] can offer background subtraction at the cost of long integration times. Single-pulse coherent control approaches[4] suppress the nonresonant background but are limited by the bandwidth of the femtosecond source to low-frequency vibrations. Interferometric CARS, while providing increased sensitivity,[5,6] can suffer from image artifacts arising from the variable index of refraction across a sample.

In this Letter we describe a new approach to enhance the vibrational contrast and sensitivity of CARS imaging. Consider an isolated resonance centered at vibrational frequency Ω_R with FWHM linewidth Γ (Fig. 1a) probed with a narrowband source. If the source is rapidly switched between two frequencies, ω_1 and ω_2, with a frequency difference $\delta=\omega_1-\omega_2$, this frequency modulation results in an amplitude modulation of the CARS signal, $\Delta I(\delta)=I(\omega_1)-I(\omega_2)$, that can be extracted by using lock-in detection. In this approach, a resonant spectral feature becomes a frequency modulation (FM) to amplitude modulation (AM) converter (Fig. 1b). The nonresonant contribution, which is essentially spectrally flat, does not contribute to the detected modulated signal and therefore is efficiently suppressed. The above approach is implemented by modulating at a high enough rate (>500 kHz) to separate the modulated signal from the lower-frequency laser noise. Temporal phase modulation of single broadband pulses can also give amplitude modulated CARS signals,[7] but the low modulation rates (~2–3 kHz) are not ideal for microscopy.

In this FM CARS approach, the quadratic term in relation (1) dominates at high concentration of resonant species. At much lower concentrations, however, the linear term, $2\,\mathrm{Re}\{\chi_R^{(3)}(\Omega)\}\chi_{NR}^{(3)}$, becomes more important. This heterodyne term contains a factor of $\chi_{NR}^{(3)}$, which implies that the component can be enhanced by the nonresonant response of the solvent. This signal enhancement is dependent on the Raman shift because of the line shape of $\mathrm{Re}\{\chi_R^{(3)}(\Omega)\}$ (Fig. 1a) and can be selected by properly choosing the modulation wavelengths. As in normal CARS microscopy, the value of the nonresonant contribution can vary throughout a heterogeneous sample, potentially introducing intensity artifacts. By selecting the modulation wavelengths to be $\Omega_R\pm\Gamma/2$, the linear term can be efficiently suppressed,[8] making quantitative measurements possible.

0146-9592/06/121872-3/$15.00

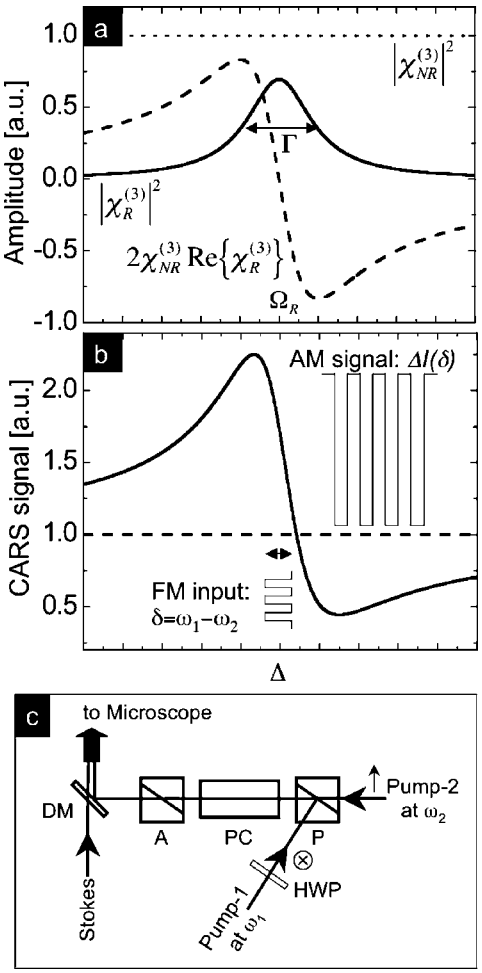

Fig. 1. a, Components of the CARS signal. The last three terms in relation (1) are plotted versus detuning $\Delta=\omega_p-\omega_s-\Omega_R$. Ω_R is the center frequency of a homogeneously broadened Raman line with linewidth Γ. The curves are calculated with an assumption that $\chi_{NR}^{(3)}=1.2\times\chi_R^{(3)}(\Delta=0)$. b, Schematic of the FM CARS process. Solid curve, sum of the contributions from a. Dashed curve, nonresonant background. The resonance acts as an FM-to-AM converter, resulting in an amplitude-modulated signal that can be detected by using a lock-in amplifier. c, Schematic of the experimental setup. PC, Pockels cell; P, two-port Glan–Taylor prism; A, Glan–Thompson prism; DM, dichroic mirror, HWP, $\lambda/2$ plate. A circled cross and an arrow indicate Pump-1 and Pump-2 polarizations, respectively.

The experimental apparatus (Fig. 1c) consists of three pulsed lasers coupled into a modified laser-scanning microscope (Olympus, FV300). The Stokes beam is ~10% of the output from a Nd:YVO_4 laser (High-Q, picoTRAIN, 7 ps, 1064 nm, 76 MHz repetition rate). The remaining 90% is used to synchronously pump an intracavity-doubled optical parametric oscillator (APE-Berlin, Levante), producing tunable 5 ps near-IR radiation for use as a pump beam (Pump-1). The second pump beam (Pump-2) is provided by a mode-locked Ti:sapphire oscillator (Coherent, Mira 900D) delivering tunable 3 ps pulses electronically synchronized[1] to the Nd:YVO_4 source. A $\lambda/2$ plate in the Pump-1 beam path rotates the polarization so that Pump-1 and Pump-2 are perpendicularly polarized. The two pump beams are combined in a two-port Glan–Taylor prism and sent collinearly into a Pockels cell (ConOptics, Model 350-160). The Pockels cell is driven by a square modulation waveform at ~500 kHz synchronized to the laser pulse train. When the waveform is in the low state, Pump-1 is allowed to pass through the exit analyzer. When the waveform is in the high state, the polarization of both beams is rotated by $\pi/2$, such that Pump-2 now passes though the analyzer while Pump-1 is blocked. The modulated pump beams are combined with the Stokes beam on a dichroic mirror and directed into the microscope. The CARS signal from the sample is detected by a photomultiplier tube (Hamamatsu, R3896) and fed into a lock-in amplifier (Stanford Research Systems, Model 844) referenced to the modulation frequency. The intensity of the two pump beams can be adjusted for maximum nonresonant signal suppression.

FM CARS is most advantageous when the resonant signal is comparable with or smaller than the nonresonant background. Figures 2a–2d show normal forward CARS and FM CARS images of weakly scattering 0.36 μm polystyrene beads on a glass surface. Pump-1 is tuned to the peak of the vinyl CH stretching band at 3050 cm^{-1}, while Pump-2 targets the spectrally flat region at 3000 cm^{-1}. The forward CARS image at 3050 cm^{-1} (Fig. 2a) shows a resonant signal only slightly above the nonresonant background, while the corresponding FM CARS image (Fig. 2c) demonstrates considerably better contrast

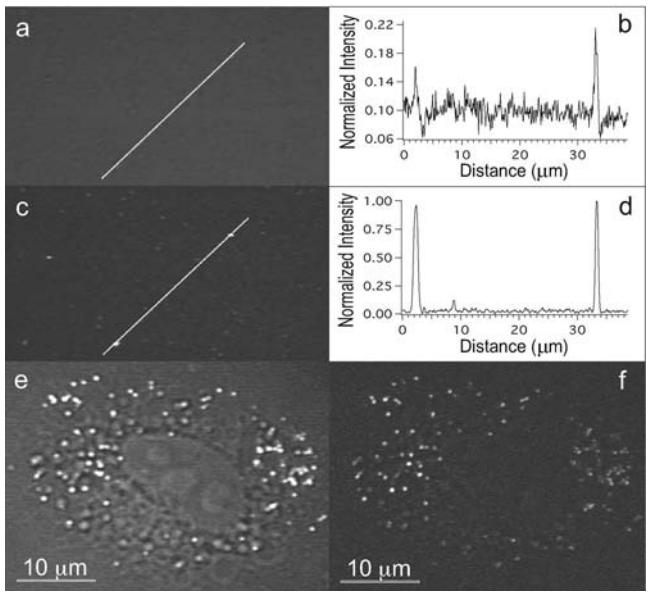

Fig. 2. Forward CARS microscopy image, a, of 0.36 μm diameter polystyrene beads taken at $\Delta=3050$ cm^{-1}. c, FM CARS image of the same area (Pump-1, 3050 cm^{-1}; Pump-2, 3000 cm^{-1}). b, d, Corresponding cross-sectional profiles of the images along the indicated line show the magnitude of nonresonant background suppression. e, Forward CARS image of a fixed A549 human lung cancer cell cultured with deuterium-labeled oleic acids taken at $\Delta=2100$ cm^{-1}. f, FM CARS image obtained when toggling between 2060 and 2100 cm^{-1}. Nonresonant background components have been significantly reduced by the FM CARS method.

(Figs. 2b and 2d). The nonresonant signal suppression of FM CARS is immediately applicable to biological imaging. Figures 2e and 2f are normal forward CARS and FM CARS images, respectively, of a fixed A549 human lung cancer cell cultured with deuterated oleic acid. The forward-CARS image at the CD_2 stretching frequency (Fig. 2e) exhibits many nonresonant cellular features that make it unclear which cellular components contain the deuterated compound. With the more sensitive FM CARS technique (Fig. 2f), the nonresonant signals vanish, revealing only the resonant signals of the deuterated lipid droplets.

The increased detection sensitivity of FM CARS was quantified with aqueous methanol solutions. Pump-1 was tuned to target the Lorentzian-shaped symmetric CH_3 stretch ($\Gamma_{\mathrm{FWHM}} \approx 25\ \mathrm{cm}^{-1}$) of methanol[9] at 2928 cm^{-1}, while Pump-2 was tuned to target 3048 cm^{-1}, where there is no resonance. At low concentrations, the FM CARS intensity, $I(\Delta, n)$, can be expressed in terms of the dilution factor n by

$$I(\Delta, n) = I^{\mathrm{H_2O}} \left[\frac{(\Gamma/2)^2}{\Delta^2 + (\Gamma/2)^2} \right] \left[Rn^2 - 2\sqrt{R} \left(\frac{2\Delta}{\Gamma} \right) n \right], \quad (2)$$

where $I^{\mathrm{H_2O}}$ is the nonresonant CARS intensity from pure water and R is the ratio of the peak CARS signal from pure methanol to $I^{\mathrm{H_2O}}$. The R parameter can be readily measured experimentally at the resonance maximum ($R = 24$ in this case).

The FM CARS signal is plotted as a function of the dilution factor in Fig. 3 for two lock-in detection bandwidths. Equation (2) provides a direct fit to the data (solid line). With a lock-in amplifier, the noise floor for the detected resonant signal can be reduced by narrowing the detector bandwidth to achieve better sensitivity. While a bandwidth of 25 kHz (filled circles) achieves significantly higher sensitivity than normal CARS, the lowest concentration measured in the experiment is obtained at a detection bandwidth of 1.6 Hz (open circles). At this limit, FM CARS allowed for the detection of 5×10^5 oscillators in the probed volume of ~ 100 al as compared with 4×10^8 oscillators with normal forward CARS in the same experiment. We observe that the minimum detectable signal does not scale linearly with the lock-in bandwidth. This suggests that the CARS signal noise spectrum has significant components in the subhertz region, which most likely originate from beam pointing instabilities as well as laser intensity and spatial mode fluctuations.

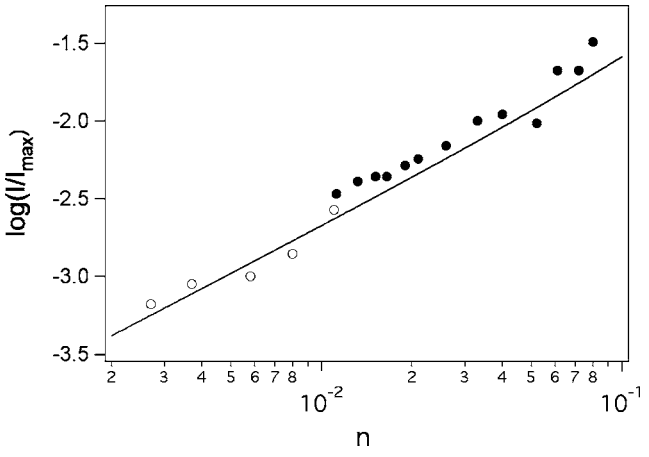

Fig. 3. FM CARS signal versus dilution factor, n. I is the FM CARS signal intensity from methanol dissolved in water, while I_{max} is the CARS signal intensity from a pure methanol sample. Filled circles represent the experimental data points taken at a detector bandwidth of 25 kHz. Open circles correspond to data taken when the detector bandwidth was set to 1.6 Hz. The solid line is a plot of Eq. (2).

Improvements to this technique, including the use of dual-wavelength, optical parametric oscillators[10] will very likely improve the detection limit by eliminating noise from the laser source. This technique can also be used to detect small changes in a vibrational band through appropriate choice of the modulated wavelengths.

In conclusion, we have demonstrated a new method for CARS microscopy that efficiently suppresses nonresonant signals based on rapid modulation of the difference frequency between the pump and the Stokes beams. This approach dramatically enhances our ability to distinguish resonant features from the nonresonant background, providing resonant images with an improvement of nearly 3 orders of magnitude in sensitivity for chemical species at low concentrations.

We thank Wei Yuan Yang for providing the A549 cells. This research was funded by a National Institutes of Health Pioneer Award to X. S. Xie. C. L. Evans acknowledges the National Science Foundation for a Graduate Research Fellowship. X. S. Xie's email address is xie@chemistry.harvard.edu.

References

1. J. X. Cheng and X. S. Xie, J. Phys. Chem. B **108**, 827 (2004).
2. C. L. Evans, E. O. Potma, M. Pourgish'haag, D. Côté, C. P. Lin, and X. S. Xie, Proc. Natl. Acad. Sci. U.S.A. **102**, 16807 (2005).
3. X. L. Nan, J. X. Cheng, and X. S. Xie, J. Lipid Res. **44**, 2202 (2003).
4. N. Dudovich, D. Oron, and Y. Silberberg, Nature **418**, 512 (2002).
5. D. Oron, N. Dudovich, and Y. Silberberg, Phys. Rev. Lett. **89**, 273001 (2002).
6. E. O. Potma, C. L. Evans, and X. S. Xie, Opt. Lett. **31**, 241 (2006).
7. E. Frumker, D. Oron, D. Mandelik, and Y. Silberberg, Opt. Lett. **29**, 890 (2004).
8. L. Li, H. Wang, and J. X. Cheng, Biophys. J. **89**, 3480 (2005).
9. M. Schwartz, A. Moradi-Araghi, and W. H. Koehler, J. Mol. Struct. **63**, 279 (1980).
10. F. Ganikhanov, S. Carrasco, X. S. Xie, M. Katz, W. Steitz, and D. Kopf, Opt. Lett. **31**, 1292 (2006).